Journal of Visualization, Vol. 8, No. 3 (2005)269-276

Performance of a PIV System for a Combusting Flow and Its Application to a Spray Combustor Model

Kiuchi, M.*[1], Fujisawa, N.*[1]and Tomimatsu, S.*[2]

*1 Department of Mechanical Engineering, Niigata University, 8050 Ikarashi-2, Niigata, 950-2181, Japan. E-mail: fujisawa@eng.niigata-u.ac.jp
*2 R&D Center, DMW Corporation, 3-27, Miyoshi, Mishima, Shizuoka, 411-8560, Japan.

Received 28 October 2004
Revised 23 February 2005

Abstract : The performance of PIV system for combusting flow was evaluated by using artificial images generated from computer graphics and experimental data. The influences of shutter speed, filter, laser power and the PIV algorithms on the measurement uncertainty were studied for optimizing the performance of the PIV system. This system was applied to the spray combustor model for boiler, and the flow patterns with and without combustion were elucidated. Results showed that the burner flow generates complex three-dimensional flow pattern, which contributes to highly mixed fuel flow in the combustor. Although the flow pattern with and without combustion is similar, the growth of burner flow area and an increase in velocity magnitude are found in the flow field by the influence of chemical reactions in combustion.

Keywords : Visualization, PIV, Combustion, Flame, Spray, Combustor.

1. Introduction

The velocity measurement of combustion flow has been a topic of interest for many years because of the importance in designing highly-efficient combustors. Such combustion flow has been measured by using Laser Doppler Anemometry (LDA) and Particle Image Velocimetry (PIV). The latter technique is becoming more important for velocity measurement, because it allows whole-flow measurement of instantaneous velocity field in the combustion flow (Kawanabe et al., 2000, Stella et al., 2001 and Chinone and Fujisawa, 2004).

When the sprayed fuel is combusted, a luminous flame appears inside the chamber due to the generation of soot particles in the flame. The velocity field then becomes more difficult to measure with a standard PIV system, because the captured images suffer from the influence of this high intensity of the luminous flame. Therefore, the light emitted from the luminous flame has to be removed in order to capture clear images of the tracers necessary for PIV processing. In order to overcome this difficulty, the imaging technique by the standard PIV system has been improved by using the high-speed shutters (Shioji et al., 1997), band-pass filers (Ikeda et al., 2000, Palero and Ikeda, 2002, Chinone and Fujisawa, 2004) and combined use of rotary shutters and band-pass filters (Willert and Jarius 2002, Fujisawa et al., 2003, Tomimatsu et al., 2003). By weakening the influence of the high-intensity luminous flame by these additions, it is made possible to evaluate the velocity field by PIV. However, the influence of these additions on the uncertainty of velocity measurement has not been understood in the present state of the art.

Information on the three-dimensional flow pattern in the combustor is very important in optimizing the combustor geometry. However, there have not yet been reported on such flow field in combustors, which seems mainly to be due to the difficulty of measuring a flow in the presence of a luminous flame. Tomimatsu et al. (2003) have measured a two-dimensional velocity field in a spray combustor model with combustion, but their results were limited to the central plane in the combustor model. In order to clearly understand the details of the flow field, the measurements must also be made on the three-dimensional flow in such a model as well.

The purpose of this paper is therefore to evaluate the performance of a PIV system for combustion flow using the artificial images, and attempt to find optimal system parameters, such as the shutter speed, band-width of filter, laser power and the PIV algorithms. Further, the PIV system is applied to the three-dimensional flow in the spray combustor model, in order to understand the flow dynamics in the combustor, both with and without combustion.

2. Experimental Setup

2.1 Combustor Model

The experimental model combustor used in the present study is shown in Fig. 1. The height of this model was 161 mm, with a horizontal area 105 mm × 105 mm, being therefore a 1/5 scale model of the domestic boiler combustor. The top and bottom plates, and the side plate supporting the burner, were made of iron, while the other three sides plates were made of heat-resistant glass, in order to have visual access to the flow in the combustor. Kerosene fuel was sprayed from the burner nozzle at a spray angle of 68 deg and the air was supplied by a blower. A baffle plate attached to the spray nozzle generated a swirl flow to mix the air and fuel in the combustor. In the present experiment, the mass flow rate of air and fuel were 4.3 g/s and 0.056 g/s, respectively, so that the fuel air ratio was 77. The air velocity U_0 at the burner exit was set to 1.4 m/s. Further details of combustor model as well as the experimental conditions have been described in Tomimatsu et al. (2003).

2.2 PIV Measurements

Flow visualization of combustion flow is carried out with hollow silica particles of 2 μm diameter and 0.2 g/cm^3 density, which were selected to provide good traceability of the particles to the flow. These tracers were seeded at the inlet of the blower and supplied into the combustor.

The experimental setup is shown in Fig. 2. It consisted of a monochrome CCD cameras (1008 × 1018 pixels with 8bits in gray level) with a frame-straddling function, double-pulsed Nd:YAG

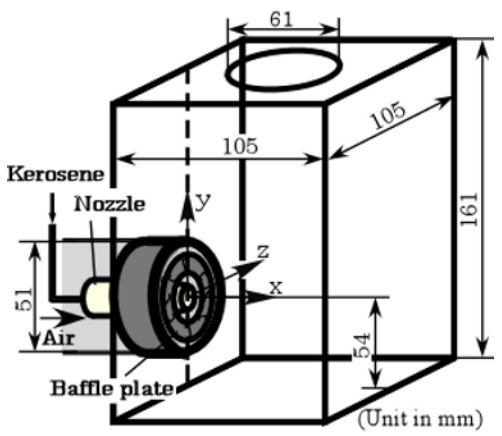

Fig. 1. Combustor model.

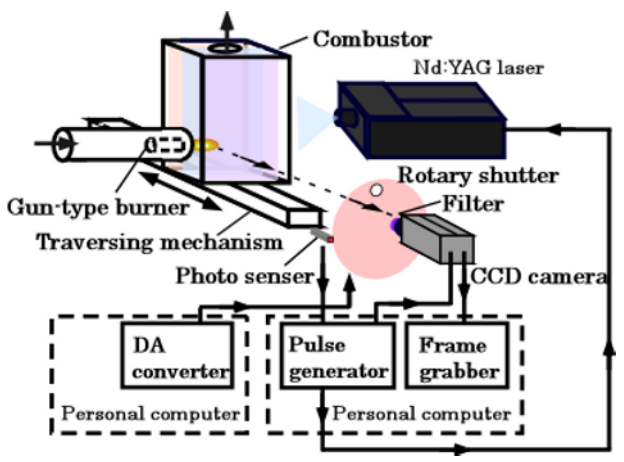

Fig. 2. PIV system for combusting flow.

lasers (50 mJ/pulse and 532 nm wavelength) and a pulse controller. Illumination was provided by a light sheet (1 mm thick) from the Nd:YAG lasers, operated at pulse interval 135 μs, with pulse width 6 ns and pulse repetition rate 15 Hz. The rotary shutter mechanism and the band-pass filter are placed in front of the CCD camera, in order to minimize the intensity of luminous flame.

The rotary shutter mechanism consists of a rotary disk driven by a DC servomotor. A photoelectric sensor in front of the disk assisted in the synchronization of the rotary shutter and the camera. Further details of this rotary shutter mechanism and the timing chart can be found in Tomimatsu et al. (2003).

PIV measurements were carried out in the combustor at 17 *x-y* and 17 *y-z* vertical planes, which allowed the evaluation of three-components of mean velocities in the flow field. (Out-of-plane velocities in *x-y* plane were obtained from the in-plane velocities in *y-z* plane and vice versa.)

A pair of particle images at every vertical plane was processed by direct cross-correlation algorithm, with interrogation window size 31 x 31 pixels and search window size 8 x 8 pixels, as this combination was found to minimize the erroneous velocity vectors while providing reasonable spatial resolution. Interrogation windows were overlapped by 50% to obtain the velocity vectors. Sub-pixel analysis was also introduced to improve the measurement accuracy. Finally, incompletely-combusted kerosene droplets were removed from the PIV images by image processing, under the principle that the light intensity of the droplets was much larger than that of the tracer particles (Tomimatsu et al., 2003).

3. Uncertainty Analysis Using Artificial Images

3.1 Generation of Artificial Images

The performance of the rotary shutter mechanism was studied using computer-generated artificial images. This approach allows for an evaluation of uncertainty in the PIV measurement, by comparing the PIV result from the artificial images and the assumed velocity field for generating the images. (For real PIV images with combustion see Tomimatsu et al. (2003).)

Assumptions made in generating the artificial images were as follows: (1) The light sheet illuminating the flow field had a Gaussian intensity distribution. (2) Tracer particles were randomly distributed in three-dimensional flow field. (3) The tracer particles followed the velocity field. (4) The intensity of each tracer particle was expressed by Gaussian distribution. (5) The peak intensity of the particle was obtained by the experimental observation. (6) The number of tracer particles and the pixel diameter were determined by experimental observation. (7) The luminous flame noise was obtained from the experimental histogram. (8) The spatial non-uniformity of the luminous flame was not considered. Further details on the generation of artificial images can be found in Raffel et al. (1998), Fujisawa and Hashizume (2001) and Okamoto et al. (2001).

The velocity field was assumed by the following equations to simulate the main feature of the three-dimensional vortical structure in the combustor (Fig. 3(a)):

$$\begin{aligned} u &= 2U_1 \sin(2\pi x/\lambda)\cos(2\pi y/\lambda)\sin(2\pi z/\lambda) \\ v &= U_1 \cos(2\pi x/\lambda)\sin(2\pi y/\lambda)\sin(2\pi z/\lambda) \\ w &= U_1 \cos(2\pi x/\lambda)\cos(2\pi y/\lambda)\cos(2\pi z/\lambda) \end{aligned} \tag{1}$$

where u, v, w are three velocity components in x, y and z directions, respectively, λ is the wavelength of vortices, U_1 is the magnitude of velocity fluctuation.

Figure 3(b) shows the histogram of the first and second frame of the experimental images, which are taken in the luminous flame near the burner. The laser power and the band-width of filter

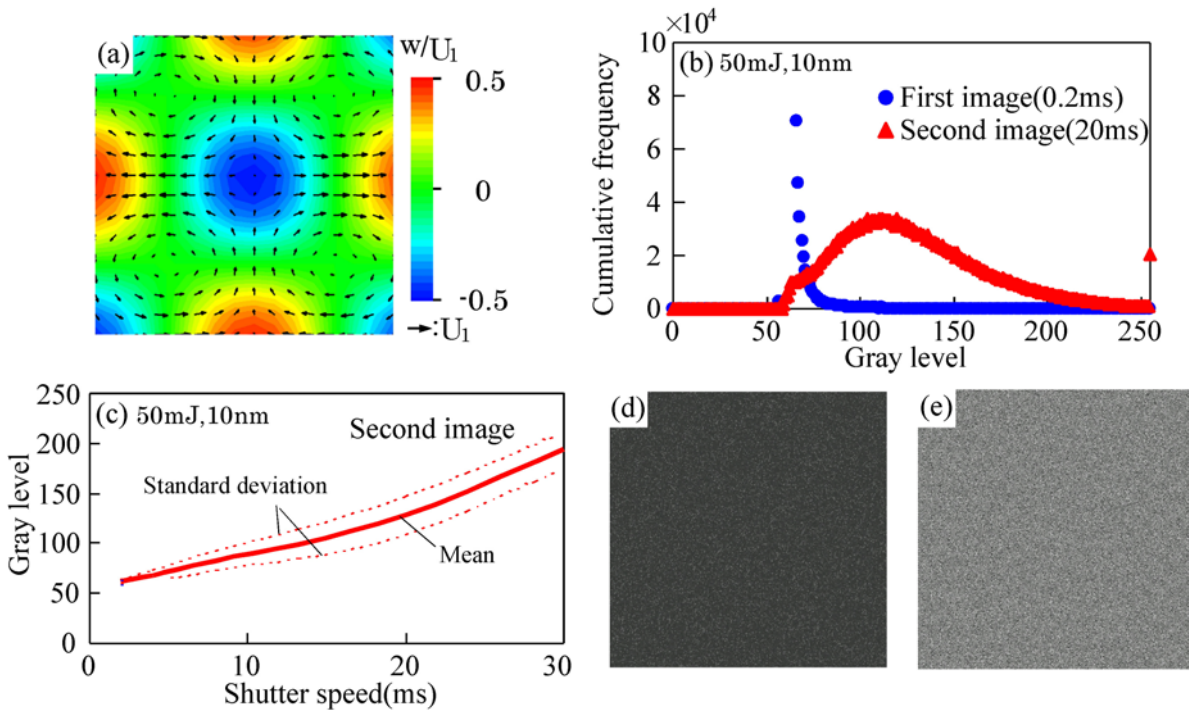

Fig. 3. Generation of artificial images: (a) Velocity field, (b) Histogram of images, (c) Variations of gray levels with shutter speed, (d) First image (0.2 ms), (e) Second image (20 ms).

are set to 50 mJ and 10 nm, respectively. Note that the shutter speed of the first frame is fixed to 0.2 ms and that of the second frame is 20 ms, which can be determined by the rotary shutter mechanism. Such feature of histogram is due to the integrated effect of the luminous flame, which appears randomly in the flame. In order to characterize the influence of luminous flame, the mean and the standard deviation of the histogram in the flame are evaluated, and the result is shown in Fig. 3(c). The mean and standard deviations of the histogram on the second frame are gradually increased with an increase in shutter speed, due to the influence of luminous flame. These features are reproduced in the artificial images. It should be mentioned that the mean and standard deviations of the histogram at various combinations of shutter speed, band-width of filter and laser power are obtained from the experimental result and they are reproduced in the artificial images by randomly distributing the gray level on each pixel of the image.

Figure 3(d), (e) show the examples of the first and second artificial images in the luminous flame, respectively. They are generated at the same experimental condition as shown in Fig. 3(b). The number of tracer particles is 10,000 and the average pixel diameter is set to 2 pixels. These images reflect the variations of gray level in the luminous flame caused by the change of shutter speed in the present CCD camera.

3.2 Uncertainty of PIV Measurement

The uncertainty of PIV measurement is defined as follows,

$$V_e = \frac{\sum\sqrt{(U_i - U_i^*)^2 + (V_i - V_i^*)^2}}{\sum\sqrt{U_i^{*2} + V_i^{*2}}} \tag{2}$$

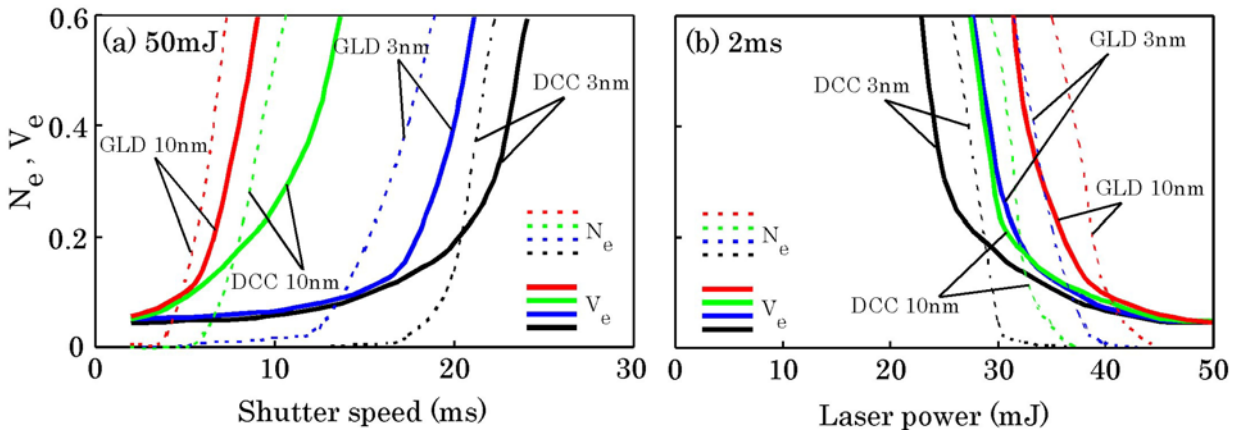

Fig. 4. Velocity uncertainties with respect to shutter speed and laser power.

where U_i, V_i are i-th in-plane velocity components among all the reference points M (where M = 17 × 17 in the present study). The quantities with * in Eq. (2) are corresponding velocities given by Eq. (1) and the quantities without * in Eq. (2) are obtained from the PIV processing of the artificial images. Note that the velocity uncertainty Ve shows a degree of uncertainty in the image analysis of PIV measurement. In the following, the uncertainty due to the influence of luminous flame was studied at various shutter speeds, filter band-widths, laser power levels and the PIV algorithms.

Figure 4 shows the velocity uncertainty Ve and the error ratio Ne of PIV measurement using the direct cross-correlation algorithm (DCC), plotted against shutter speed (Fig. 4(a)) and the laser power (Fig. 4(b)) at two different filter band-widths 3 nm and 10 nm. The error ratio Ne is defined by the number of erroneous velocity vectors, which is deviated more than 1 pixel in magnitude from the true velocity vectors, over that of whole velocity vectors. The interrogation window size was set to 31x31 pixels, the search window size to 8 x 8 pixels and the particle displacement between the two images to 4.5 pixels. These were found to be the optimum values for the PIV analysis. The results indicate that the velocity uncertainty Ve decreases with a decrease in shutter speed (Fig. 4(a)) and with an increase in laser power (Fig. 4(b)). Note that the growth of the velocity uncertainty is followed by an increase in erroneous velocity vectors. Furthermore, Ve decreases with a decrease in filter band-width. The uncertainty of PIV measurement with combustion approached Ve = 5%, when the shutter speed, the band-width of the filter and the laser power are set to 2 ms, 3 nm and 50 mJ, respectively, while the uncertainty without combustion at these settings were found to be 3%. This difference in uncertainties is responsible for the background noise under the combustion.

The PIV analysis was also carried out using the gray-level difference method (GLD) and the results are given in Fig. 4(a), (b) for comparison. Note that this algorithm was used in our previous report (Tomimatsu et al., 2003). The present results indicate that the uncertainty of PIV measurement was greatly improved by the direct cross-correlation method used in the present study. Such improvement in the uncertainty was due to the normalization of the image intensities between the two sequential images in the direct cross-correlation method, while they were not normalized in the gray-level difference method.

4. Experimental Results and Discussion

4.1 Cross-Sectional Velocity Distributions

The three-dimensional mean velocities in the combustor model with and without combustion were evaluated from the PIV measurement with rotary shutter mechanism. In the present experiment, the shutter speed of the second frame, the filter band-width and the laser power were set to 2 ms, 3 nm and 50 mJ, respectively. Figures 5 and 6 show the mean velocity distributions in x-y plane of the

combustor model with and without combustion, respectively. The positions of the measurement plane are set to z/B = 0, 0.23 and 0.40 (B : side length of test section), with out-of-plane mean velocities being evaluated from the measurement of mean velocities in y-z plane. Note that the mean velocities were obtained by averaging 150 instantaneous velocity distributions measured by PIV. The vertical velocity v in the present result is an average of two measurements, which agree with each other within ± 5% with combustion.

The mean velocity distribution with combustion at the burner center z/B = 0 (Fig. 5(a)) shows that the burner flow was generated from the burner nozzle and impinged on the counter-plate of the combustor, where the flow rolls up and down to form recirculating flows in the upper and lower chamber of the combustor, respectively. The upward flow went to the outlet at the top of the combustor, and the downward flow formed a complex flow pattern inside the chamber.

Although the flow pattern at the off-center plane z/B = 0.23 was similar to that at the burner center z/B = 0, the width of the burner flow becomes smaller and the velocity magnitude was reduced. With a further shift of measurement plane to the side-plate z/B = 0.4, the direct influence of the burner flow is weakened and the recirculating flow was magnified around the corner of the combustor. Note that the lower recirculating flow went along the bottom plate and moved upward along the burner plane through both sides of the burner. It was found that the out-of-plane velocities (indicated in Figs. 5 and 6 by a color bar) increase in the off-center planes. The positive out-of-plane velocities were generated on the burner flow and the impinging region over the counter-plate (z/B =

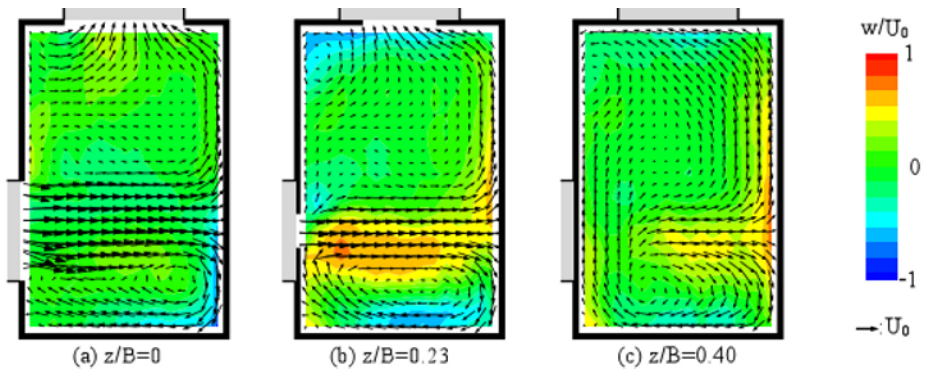

Fig. 5. Mean velocity distribution in combustor with combustion.

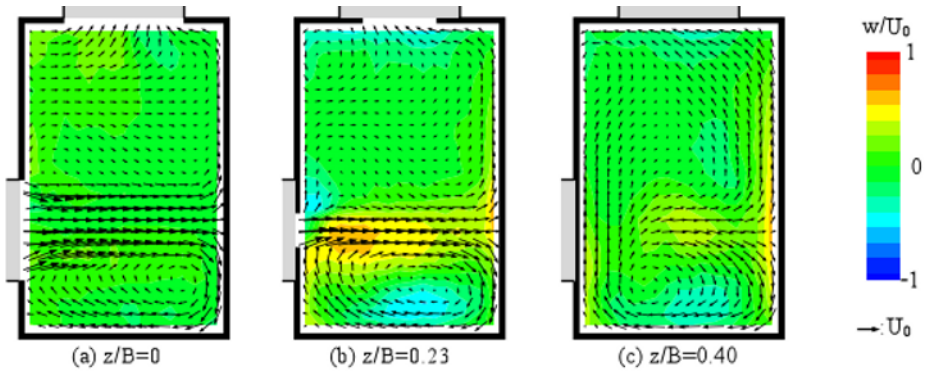

Fig. 6. Mean velocity distribution in combustor without combustion.

0.23), while the lower recirculating flow shows the negative out-of-plane velocities. A swirl flow is therefore generated in the lower recirculation region. Although this swirl flow weakened near the side-plate (z/B = 0.4), positive out-of-plane velocities were still large over the counter-plate due to the presence of secondary flow over the side-plates.

The mean velocity distribution without combustion at various cross-sectional planes is shown in Fig. 6. Although the flow patterns in the combustor are very similar to those with combustion in

Fig. 5, the width of the burner flow is reduced, and the velocity magnitude of the burner flow and the out-of-plane velocities were reduced in comparison with the combustion. These differences in flow field with and without combustion can be due to the influence of chemical reactions in combustion.

4.2 Three-Dimensional Flow Pattern

The streamlines and the three-dimensional flow pattern of the combustion flow are shown in Fig. 7, obtained from all the velocity measurements in *x-y* and *y-z* planes of the combustor. It was clearly seen that the burner flow generated upper and lower recirculating flows, due to its impinging on the counter-plate of the combustor. Although the upper recirculating flow goes directly to the combustor outlet, the lower recirculating flow goes through the burner side and approaches the outlet along the burner-plate. Such three-dimensional flow entrains the surrounding air into the burner flow and enhances the mixing of the fuel and air in the combustor due to its highly turbulent flow pattern, resulting in high-performance combustion.

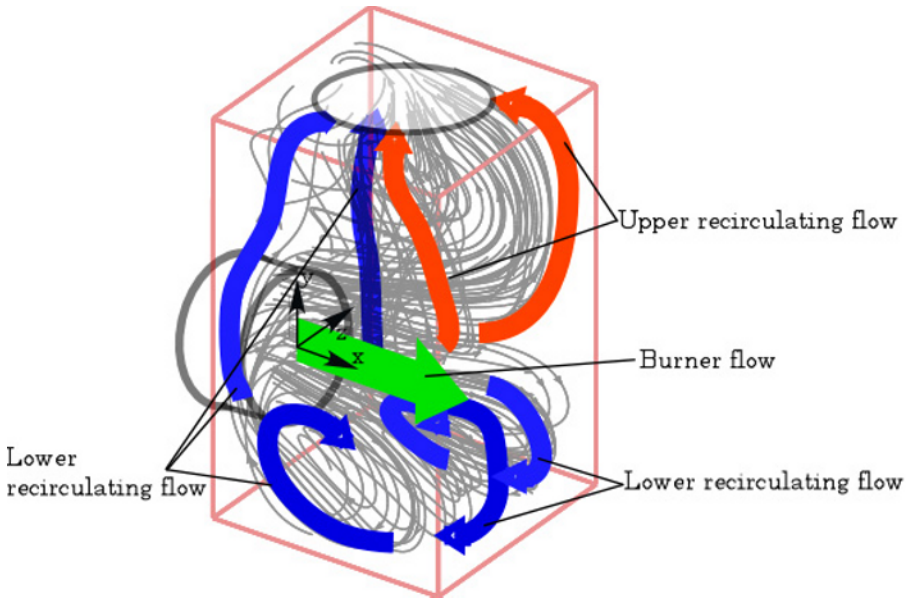

Fig. 7. Tree-dimensional distributions of streamlines with combustion.

5. Conclusion

Using the artificial images, the uncertainty of PIV measurement of velocity field in spray combustion was studied for optimizing the PIV system with rotary shutter mechanism. Results indicated an optimum configuration of the PIV system for application to the combustion flow with luminous flame. Satisfactory accuracy in PIV measurement was obtained at certain combinations of shutter speed, filter band-width and laser power, in conjunction with the direct cross-correlation PIV algorithm. Further, three-dimensional measurement of the combustion flow in a combustor model was conducted by the PIV system, in order to elucidate the flow mechanism. It was found that the impingement of the burner flow on the counter-plate generates a three-dimensional flow field with upper and lower recirculating flow. Such a complex flow pattern in the combustor enhances the highly mixing of fuel and air in the combustor, resulting in high-performance combustion.

Acknowledgements

The authors appreciate the technical suggestion by Mr. Tokita, Y., Corona Corporation.

References

Chinone, S. and Fujisawa, N., Visualization of Dilute Hydrogen Jet Flame in Air Flow, Journal of Visualization, 7 (2004), 291-298.

Fujisawa, N. and Hashizume, Y., An Uncertainty Analysis of Temperature and Velocity Measured by a Liquid Crystal Visualization Technique, Measurement Science and Technology, 12 (2001), 1235-1242.

Fujisawa, N., Hosokawa, A. and Tomimatsu, S., Simultaneous Measurement of Droplet Size and Velocity Field by an Interferometric Imaging Technique in Spray Combustion, Measurement Science and Technology, 14 (2003), 1341-1349.

Ikeda, Y., Yamada, N. and Nakajima, T., Multi-intensity-layer Particle-image Velocimetry for Spray Measurement, Measurement Science and Technology, 11 (2000), 617-626.

Kawanabe, H., Kawasaki, K. and Shioji, M., Gas-flow Measurements in a Jet Flame Using Cross-correlation of High-speed-particle Images, Measurement Science and Technology, 11 (2000), 627-632.

Okamoto, K., Nishio, S., Kobayashi, T., Saga, T. and Takehara, K., Evaluation of the 3D-PIV Standard Images (PIV-STD Project), Journal of Visualization, 3 (2001), 115-123.

Palero, V. and Ikeda, Y., 3D Imaging of Evaporating Fuel Droplets by Stereoscopic PIV, Journal of Visualization, 5 (2002), 285-292.

Raffel, M., Willert, C.E. and Kompenhans, J., Particle Image Velocimetry, (1998), 134-146, Springer, Berlin.

Shioji, M., Kawanabe, H. and Ikegami, I., PIV Measurement of Gas Flows in a Jet Flame, Proc. 1st Asia-Pacific Conference on Combustion (Osaka), (1997), 306-309.

Stella, A., Guj, G., Kompenhans, J., Raffel, M., Richard, H., Application of Particle Image Velocimetry to Combusting Flows: Design Considerations and Uncertainty Assessment, Experiments in Fluids, 30 (2001), 167-180.

Tomimatsu, S., Fujisawa, N. and Hosokawa, A., PIV Measurement of Velocity Field in a Spray Combustor, Journal of Visualization, 6 (2003), 273-281.

Tomimatsu, S, Fujisawa, N. and Kiuchi, M., Uncertainty Analysis of PIV Measurement of Flow in Luminous Flame Using Artificial Image, Proc. 11th Int. Symp. Flow Visualization (South Bend), (2004), paper 3.1.1.

Willert, C. and Jarius, M., Planar Flow Field Measurements in Atmospheric and Pressurized Combustion Chambers, Experiments in Fluids, 33 (2002), 931-939.

Author Profile

Masaya Kiuchi: Graduate School of Niigata University (M.E. 2005); now working at Suzuki Corporation.

Nobuyuki Fujisawa: Tohoku University (D.E. 1983); joined Gunma University in 1983; Associate professor; 1991. Professor, Niigata University, 1997. Principal research field: visualization, non-intrusive measurement and control of thermal and fluid flow phenomenon in mechanical engineering.

Shigeyuki Tomimatsu: Graduate School of Kansai University (M.E. 2000), Graduate School of Niigata University (D.E. 2004). Research and Development Center at DMW Corporation (2003). Research interests: computational fluid dynamics and quantitative flow visualization for fluid machinery.